

Absorption-based Quantum Communication with NV centres

Burkhard Scharfenberger¹, Hideo Kosaka², William J. Munro^{3,1} and Kae Nemoto¹
¹ *National Institute of Informatics, 2-1-2 Hitotsubashi, Chiyoda-ku, Tokyo 101-8430, Japan*

² *Department of Physics, Yokohama National University,
Sogo-Kenkyuto S306, Tokiwadai, Hodogayaku, 240-8501 Yokohama, Japan and*

³ *NTT Basic Research Laboratories, NTT Corporation,
3-1 Morinosato Wakamiya, Atsugi, Kanagawa 243-0198, Japan*

(Dated: July 1, 2015)

We propose a scheme for performing an entanglement-swapping operation within a quantum communications hub (a Bell like measurement) using an NV- centre's $|\pm 1\rangle \leftrightarrow |A_2\rangle$ optical transition. This is based on the heralded absorption of a photon resonant with that transition. The quantum efficiency of a single photon absorption is low but can be improved by placing the NV center inside a micro cavity to boost the interaction time and further by recycling the leaked photon back into the cavity after flipping its phase and/or polarisation. Throughout this process, the NV is repeatedly monitored via a QND measurement that heralds whether or not the photon absorption has succeeded. Upon success we know a destructive Bell measurement has occurred between that photon and NV center. Given low losses and a high per-pass absorption probability, this scheme allows the total success probability to approach unity. With long electron spin coherence times possible at low temperatures, this component could be useful within a memory-based quantum repeater or relay.

I. INTRODUCTION

Quantum communication [1–5] is a resource that will be required in the development of tomorrow's quantum internet [6] whether it be to share quantum enabled information over short, medium or long ranges. It will enable a multitude of tasks ranging from quantum key distribution (QKD) [4], device independent QKD [7] to distributed quantum computation and sensing [8–10]. Especially over long ranges (hundreds or thousands of kilometres) one will require shared entanglement to enable this, which will most likely require the use of quantum repeaters [11–13]. These take the form of a chain of nodes able to perform two basic functions: the first being to store already established entangled links between nodes and the second to merge two links into a new, longer one. Many repeater schemes using various approaches to provide this functionality and various physical systems to implement the nodes of such a repeater have been put forward over the years [2, 3, 12–26], including negatively charged nitrogen vacancy center in diamond (NV-) [27, 28].

The NV- center is made up of a vacant carbon position in a diamond lattice adjacent to a substitutional nitrogen atom [29–32] has many desirable properties [27, 33–39], including long coherence times [37] and good controllability of both electronic and nuclear spins at different temperatures [34, 37, 39–50]. The experimentally accessible states are the ground state manifold (GSM) and the excited state manifold (ESM), both of which are spin triplets but the former is composed of orbital angular momentum singlets (A_2) while the states of latter form orbital doublets (E) under the action of the defect's symmetry group C_{3v} [32]. The two sets of states are separated by an optical transition with zero-phonon-line wavelength of 637nm [38] while a set of optically inacces-

sible intermediate spin-singlet states can be reached from the ESM via non-radiative decay processes [32].

NV- centres have already been used as emitter of two different kinds of entangled photon qubits: polarisation [51] and time-bin [52]. The former makes use of the special Bell-state like form of the four $m_S = \pm 1$ zero field ESM states. In particular the $|A_2\rangle$ state does not couple to the intermediate singlet states. Since in a dipole interaction the z-component of total the angular momentum must change by ± 1 , spontaneous emission out of $|A_2\rangle$ creates a photon which is polarisation-entangled with the two degenerate $m_S = \pm 1$ states of the GSM [38]. It has been recently demonstrated experimentally, that the time reversal also holds: absorption of a photon acts like a projection onto a joint photon-vacancy spin Bell-state [53]. In principle this could allow for the teleportation of quantum information from an incoming photon to any qubit the absorbing NV- is entangled with.

Our proposal is to use this feature of the NV center as a core element of a quantum communications network. A node in the network can perform an entanglement swap operation upon heralded absorption of a photon carrying an entangling link to a remote NV-. The heralding (QND type) measurement is implemented via detecting the phonon-side band photons of a classical laser pulse tuned to the transition between the $m_S = 0$ state of GSM and ESM after a microwave π -pulse resonant with the $|A_2\rangle$ to $|E_{x|y}\rangle$ ($m_S = 0$) transition. To enhance interaction, the NV- would be placed inside a micro cavity but even in this case the single-pass absorption quantum efficiency would be limited to 25%. We can however increase this further by adding a fibre-optic loop to re-cycle leaked photons back into the cavity after potentially flipping its phase and/or polarisation.

This paper is structured as follows: in section II we describe the main idea of the entanglement swapping

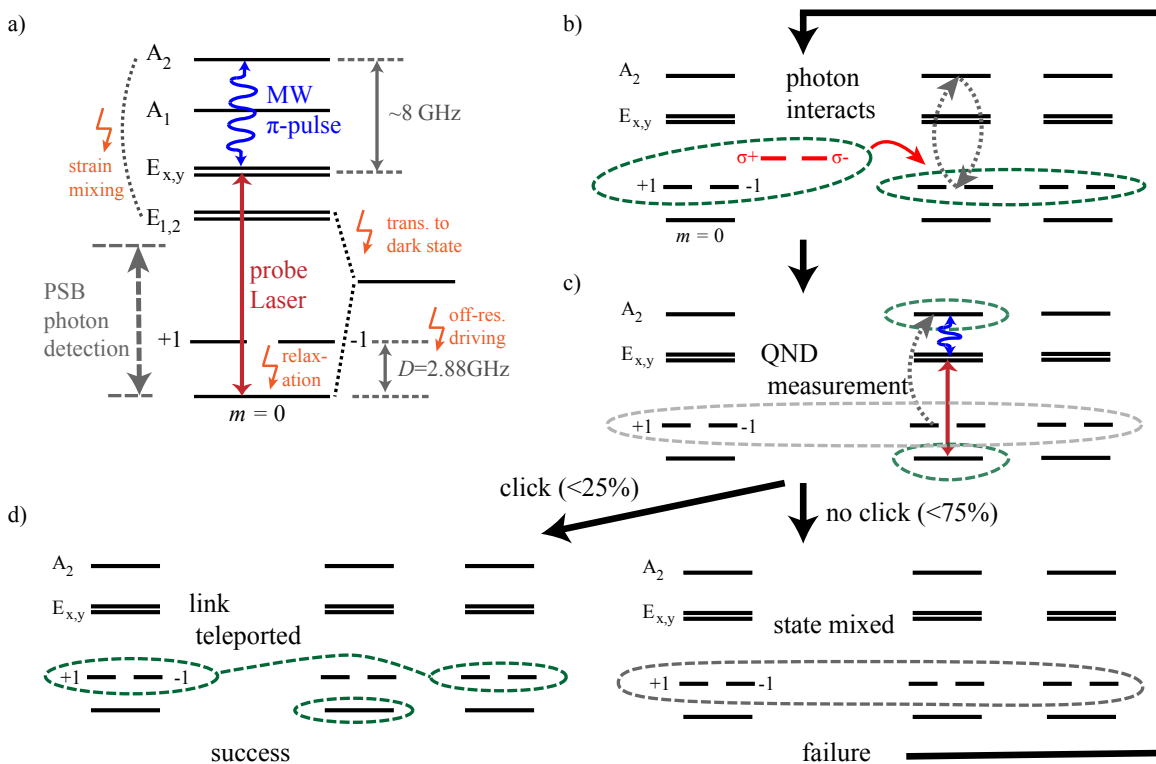


FIG. 1: An illustration of the QND measurement and its use in teleportation. a) QND measurement and potential error channels (orange symbols). Off-resonant driving can be strongly suppressed by timing the length of the π -pulse. b) a spontaneously emitted photon entangled with the left NV travels to and interacts with the NV in the middle, which is entangled with a third NV, causing coherent oscillations between $|\pm 1\rangle$ and $|A_2\rangle$. c) when the amplitude of $|A_2\rangle$ is maximal (within the photon residence time τ_{int}) the QND measurement is applied d) receiving PSB photons ('click') heralds projection onto $|A_2\rangle$ and teleportation of the entangled link. If no signal is seen within some time window, the state has become completely mixed (assuming the photon actually interacted)

scheme, detailing two possible approaches to increase quantum efficiency beyond 25%. We then proceed in In section III to present a model of the scheme as a discrete-time Quantum Markov process including estimations for the various parameters appearing. We show the results of numerical simulations using this model for different parameter regimes, allowing us to make quantitative statements about the expected performance of our scheme taking into account losses and errors. In section IV we briefly discuss how this heralded Bell measurements can be used in quantum repeaters and relays. We summarise our findings in section V.

II. TELEPORTATION SCHEME

Here we will describe in detail the three main ingredients of our scheme, the entangling absorption operation, the QND measurement and photon recycling.

Entangling absorption. — At zero magnetic field and zero strain the ESM A_2 state has the form $|A_2\rangle = (|E_+, -1\rangle + |E_-, +1\rangle)/\sqrt{2}$ where E_{\pm} and ± 1 denote the (collective) orbital angular momentum and spin of the

NV^- vacancy respectively. This is a ψ_+ Bell state between the orbital and spin degree of freedoms. From this $|A_2\rangle$ state there are dipole-allowed optical transitions to the GSM $m_S = \pm 1$ states which due to angular momentum conservation are dependant on the photon polarisation.

This property of the A_2 state was exploited in [51] to generate polarisation-entangled photons by spontaneous emission out of the $|A_2\rangle$ state. However, this 'entangling emission', can also be time-reversed into an 'entangling absorption' of an incoming photon. As was demonstrated in a recent experiment absorption into $|A_2\rangle$ is equivalent to a Bell-measurement on the joint photon-vacancy electronic spin system of the form [53]

$$M_{\psi_{\pm}} = \frac{1}{2} (|+1, \sigma_{-}\rangle + |-1, \sigma_{+}\rangle) \langle \langle +1, \sigma_{-} | + \langle -1, \sigma_{+} | \rangle \quad (1)$$

where the first quantum number refers to the vacancy spin and the second to the circular photon polarisation states σ_{\pm} . This implies, that if the absorbing NV centre starts out maximally entangled with some other qubit, whatever information the photon was carrying will be teleported to that qubit. This is basic process which enables our proposed quantum repeaters and relays.

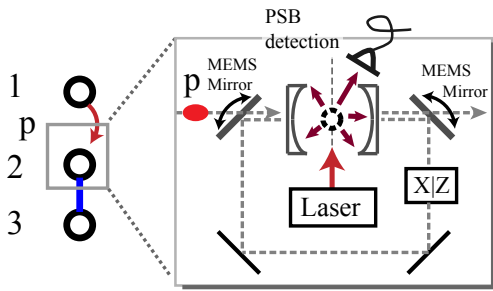


FIG. 2: Sketch of the recycling loop: a micro cavity enhances NV photon interaction in order to get a higher absorption probability per pass. Since manipulating the NV is not possible while the QND measurement is on the photon state. This is done outside the cavity by either actively (approach A) or passively (approach B) flipping the photon's phase/polarisation before sending it back into the cavity.

QND measurement. — It is important to realise, however, that the teleportation does not happen until NV centre is detected in the $|A_2\rangle$, i.e. until the state is projected onto $|A_2\rangle$. Without this, the interaction with the photon will simply cause coherent flip-flops between the NV's initial state (locally a completely mixed state of $m_S = \pm 1$) and $|A_2\rangle$ at a frequency determined by the interaction strength. We propose to implement this projective QND measurement via a microwave π -pulse resonant with the transition from $|A_2\rangle$ to the ESM $m_S = 0$ states $|E_{x|y}\rangle$ and simultaneous irradiation with a probe laser beam tuned to the transition between the $m_S = 0$ states in the GSM and ESM ($\approx 637\text{nm}$). Detection of phonon-side-band (PSB) photons would then herald, that the NV indeed was in $|A_2\rangle$, while seeing no signal can with high confidence be interpreted to mean the system is still in its initial state. A schematic of the QND measurement and how it is employed as part of the teleportation scheme is depicted in figure 1. In addition to the ideal process, 1a also shows possible error channels which limit the fidelity of the QND measurement, causing either false positive (off-resonant driving, relaxation) or indeterminate errors (strain mixing plus transition to dark state). We should point out, that since the measurement is projective, the wave function changes not only in the desired case of seeing a heralding signal. Rather, also in the case where no signal is received a change has occurred, given the photon actually interacted, which can be described by the operator $1 - M_{\psi_+}$ with M_{ψ_+} the entangling measurement operator from above. The application of the QND measurement π pulse would be timed to coincide with the time of maximum probability to find the NV in $|A_2\rangle$. This is going yield quite low probabilities of absorption for a free photon pass. Therefore, we envision to place the NV inside a micro cavity which both enhances interaction strength and interaction time (residence time) between photon and NV. The cavity would have to be carefully designed to fulfil this purpose while at the same time allowing the photon to enter without being reflected.

Mismatch problem and recycling loop. — However, even with perfect absorption the incoming photon will only be absorbed at most 25% of the time if no further measures are taken. This is easily understood by looking at the full initial state $|\psi_0\rangle = \frac{1}{2}(|+1, \sigma_- \rangle + |-1, \sigma_+ \rangle)_{1p}(|+1, +1 \rangle + |-1, -1 \rangle)_{23}$, where '2' labels the NV the photon p interacts with and 1 and 3 are remote qubits, which in the following we will always assume to be other NV centres. Rewriting $|\psi_0\rangle$ in the Bell-basis between qubits 1 and 3 we find

$$|\psi_0\rangle = \frac{1}{2} \left(|\phi_+\rangle_{13} |\psi_+\rangle_{2p} + |\phi_-\rangle_{13} |\psi_-\rangle_{2p} + |\psi_+\rangle_{13} |\phi_+\rangle_{2p} + |\psi_-\rangle_{13} |\phi_-\rangle_{2p} \right). \quad (2)$$

where the $|\phi_{\pm}\rangle$ and $|\psi_{\pm}\rangle$ denote the even and odd parity Bell-states respectively. Only the $|\psi_-\rangle_{2p}$ -term allows a dipole transition to $|A_2\rangle_2$, the dipole operator matrix elements $\langle x | \vec{E} \cdot \vec{r} | A_2 \rangle$ for the three other states ($x = \psi_+, \phi_{\pm}$) are zero. Their symmetry matches the other three $m_S = \pm 1$ states of the ESM, which are however detuned by at least about 3GHz resulting in a relative transition probability ratio of at worst $p_{\text{abs}, A_1} / p_{\text{abs}, A_2} < 10^{-4}$. If we want a high overall success probability we therefore need to somehow turn the other $2p$ Bell states into $|\psi_-\rangle_{2p}$ by applying some operation to either the spin or the photon. As illustrated in Figure 2, our idea to raise the quantum efficiency closer to 1 is then to let the photon interact with the NV center inside a cavity with residence time τ_{int} determined by the cavity Q-factor, and, via the QND measurement, check whether the NV has transitioned into $|A_2\rangle$. If the heralding signal is seen the link is teleported with very high probability reduced only by the probability for a false positive, which we estimate to be low (see appendix). If no heralding signal is seen within time τ_{int} we can assume, also with high probability, that no absorption occurred and the photon left the cavity after time τ_{int} . Outside the cavity, the photon would be caught by a fibre-optic loop which serves route it back into the cavity. Furthermore the loop will contain an integrated(active or passive) switch allowing us to flip the photons's polarisation, phase or both. if this 'recycling' process takes time τ_{out} , the total (average) time per cycle is $\tau = \tau_{\text{int}} + \tau_{\text{out}}$. We would repeat this procedure a predetermined number of times L , before finally abandoning the teleportation attempt. In the ideal case of perfect absorption per pass we need to re-cycle the photon only three times, corresponding to $L = 4$, to get maximal probability of success. However, in practice absorption cannot be perfect even with a cavity, and we need to recycle multiple times per polarisation/phase setting.

A. Two approaches

Within the framework described above there are, at least, two ways of solving the mismatch problem: the

technically simpler one, which we will call approach A, is to flip only either the phase or polarisation on each cycle. After an even number $L = 2k$ of cycles without absorption we measure both the photon and the vacancy spin in the XX or ZZ basis, depending on whether we chose to flip phase or polarisation. Assuming we flip the phase, even parity outcomes ('++' or '--') correspond to a the Bell state $|\psi_+\rangle_{13}$ and odd parity ('+-' or '-+') to $|\psi_-\rangle_{13}$. As we will see later, while technically simpler to implement, this scheme requires high per-pass absorption p_{abs} to achieve good fidelities for the teleported link as well as highly efficient single photon detectors.

In another approach, here dubbed B, without these limitations both phase and polarisation are flipped periodically after l_z and l_x rounds respectively. Choosing $L = 2l_x = 4l_z$ gives each of the four possible Bell-states a (roughly) equal chance of being heralded by the QND measurement, making a final XX or ZZ measurement unnecessary. With this approach, link fidelities are almost independent of p_{abs} and decrease with the number of cycles L due to dephasing of the electronic spin, dark counts (false positive signals) and transitions to ESM states other than A_2 . It can thus be used in the low per-pass absorption probability regime but has the downsides of greater technical complexity as well as a lower total success probability p_{success} .

III. MODELLING

In this section we present a discrete time Quantum Markov model that we used to obtain quantitative results about the performance of our recycling-loop teleportation scheme when applied to a situation as shown in figure 2 taking into account real world imperfections. We restricted the description to the 32 dimensional effective Hilbert space spanned by $\{|\phi_{\pm}\rangle, |\psi_{\pm}\rangle\}_{13} \otimes \{|\phi_{\pm}\rangle, |\psi_{\pm}\rangle; |A_2\rangle, |A_1\rangle, |\pm 1\rangle\}_{2[p]}$. Starting in the state $\rho_0 = |\psi_0\rangle\langle\psi_0|$ with ψ_0 as defined in the previous section we loop through the following steps L times:

1. absorption: with probability $p_{\text{Abs}} \langle\psi_-|\rho|\psi_-\rangle_{2p}$ the photon will be absorbed and the NV transitions to the A_2 state
2. QND measurement: the NV is measured and with probability $p_{\text{click}} = p_{\text{QND}} \langle A_2|\rho|A_2\rangle_2 + p_{\text{Dark}}$ absorption is heralded, and with prob. $1 - p_{\text{click}}$ it is not. In either case the state ρ is updated accordingly
3. photon loss: with probability p_{loss} , the photon is lost during the recycling process
4. dephasing: a dephasing operation with $\eta_2 = \exp(-\tau^2/T_2^2)$ is applied to all involved NVs (1,2 and 3) in the $(|+1\rangle \pm |-1\rangle)/\sqrt{2}$ basis where τ is the time per cycle

5. flipping: every l_z -th (l_x -th) loop a phase (polarisation) flip is applied to the photon

Since imperfections in the phase and polarisation flip operations do likely not play a major role, we did not include them in this model. Furthermore, as is readily apparent, the success probability depends very strongly on the photon actually arriving at and entering into the our cavity and recycling loop structure. In fact, the chance that the photon is lost are quite high for fibre bound communications over many kilometres. However, since here we are interested only in the performance of our scheme as a component of a network we do not take this initial loss probability into account.

A. Parameter Estimation

Thus we have a total of five parameters relevant to the performance during each cycle (p_{abs} , p_{QND} , p_{Dark} , p_{loss} and η_2) and, depending on the approach (A or B), one or three more: total number of rounds L (A and B), polarisation-flip period l_x and phase-flip period l_z (only B).

For both approaches we have a fraction of false-negatives approximately $1 - p_{\text{QND}}$ of cases in which we discard a correctly teleported link (see appendix B), which is then erased when we try again. But since the QND measurement has high fidelity this is not likely to be a limiting factor.

This brings us to the question: what are realistic values for the parameters in the model? As we already stated, the QND measurement is likely to be high and the value of $p_{\text{QND}} = 99\%$ we used in our simulations is likely to be conservative. For p_{Dark} we use an equally conservative 0.01%. While a photon loss of 1dB per element is usually regarded as good, here we cannot tolerate more than $\approx 1\text{dB}$ for the total structure. We investigated values from 0 to 0.5dB but all explicit references to performance estimates are for the challenging but potentially achievable value of $p_{\text{loss}} = 0.3\text{dB}$. Furthermore, assuming a dephasing time of $T_2 = 100\mu\text{s}$ and total time per round of $\tau = 200\text{ns}$ we find that the dephasing error is about $1 - \eta_2 = 4 \times 10^{-6}$ and thus quite small.

This leaves open the probability of absorption (per pass) p_{abs} and the number of rounds L which in the next section we will treat as the variable of our analysis.

B. Analysis

With parameters as determined in the previous section, we tested multiple combinations of $p_{\text{absorption}}$ and L as well as l_x and l_z (only approach B). In the latter case the best fidelities are naturally obtained when attempts are equidistributed over all four possible Bell states between NV centres 1 and 3.

The resulting success probabilities (cumulative probability to see a heralding signal) and average link fidelities

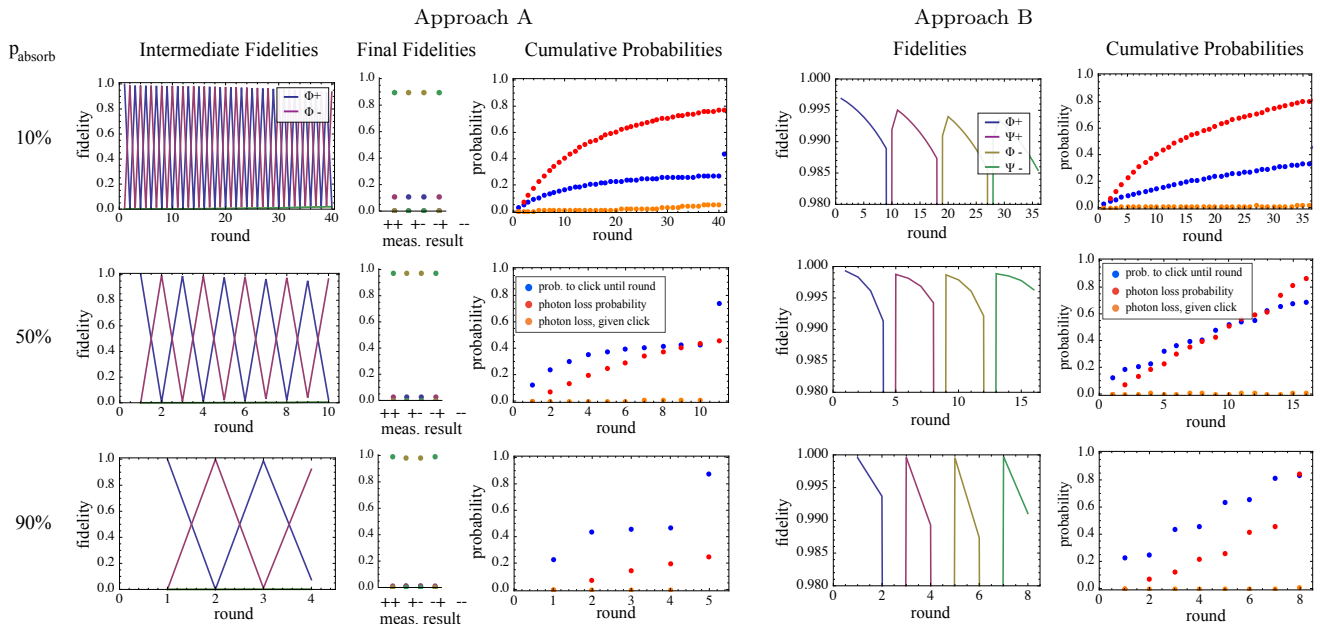


FIG. 3: Approach A and B link fidelity and success probability (=cumulative probability of seeing a click) vs number of rounds for low, medium and high absorption probability and optimal l_z , l_x (only B) and L (both). As can be seen the link fidelity declines with time mostly due to the effect of off-resonant transitions to $|A_1\rangle$.

for low, medium and high absorption probability and optimal L (and $L = 2l_x = 4l_z$ in case of approach B) are shown in figure 3 as a function of recycling round.

We find, perhaps unsurprisingly, that the probability of absorption is indeed of critical importance. However the simulations also show that there are clearly diminishing returns: the two figures of merit total success probability and average link fidelity increase much more from the low to medium p_{abs} -regime than from the medium to high regime. Consequently it seems advisable to try to increase p_{abs} to, if possible, at least around 50%, but it might not be worthwhile pushing far beyond this. At this point it is unclear, how far p_{abs} can be improved by use of a cavity, but should it prove difficult to reach or go much beyond 50% technical efforts should rather be focused on minimising the per cycle losses p_{loss} .

We also investigated the susceptibility to photon loss by performing a scan of the success probability and link fidelity for $p_{\text{absorption}}$ between 1 and 99% and per-cycle loss p_{loss} between 1 and 10%. The results, shown in figure 4, show that while at least in approach B link fidelity does not strongly depend on p_{loss} , the overall success probability quickly deteriorates with increasing p_{loss} confirming that it is indeed paramount to limit photon loss as far as possible.

Figure 4 also reveals a crossover between the two approaches A and B. While for low per-pass absorption p_{abs} , B yields superior fidelities, this advantage diminishes as p_{abs} increases and almost disappears for $p_{\text{abs}} > 90\%$, while success probability as defined here is always higher for scheme A. Thus, given the final measurement can be implemented with high reliability, approach A has a per-

formance advantage in the high p_{abs} regime, yielding an about 10% higher p_{success} at comparable link fidelity (for more detailed numbers we refer to the appendix).

IV. RELAYS AND REPEATERS

Our heralded entanglement swapping operation is an extremely useful tool for the creation of long range entangled links. As was depicted in Figure (1), this tool can be used in a relay fashion to entangle a photon emitted from a remote NV center (say at Charlie location) with an already entangled link between two other remote NV centers (at Bob and Alice respective locations). Upon a successful entanglement swapping operation, Alice and Charlie become entangled. David can then send a photon from his location to Charlie's location and the entanglement operation performed again. If it is successful, then Alice and David are entangled. In a relay fashion, longer range entanglement can be created. The probability of success for the creating this longer range links however will decrease exponentially with the numbers of nodes. However using an entangled polarisation source of photons, two separate entangled links can be merged together (as is normally done in repeater networks). This in principle allows one to avoid this exponential issue. Further the entanglement swapping operations can be used to enable entanglement purification and so one has all the necessary elements for a quantum network.

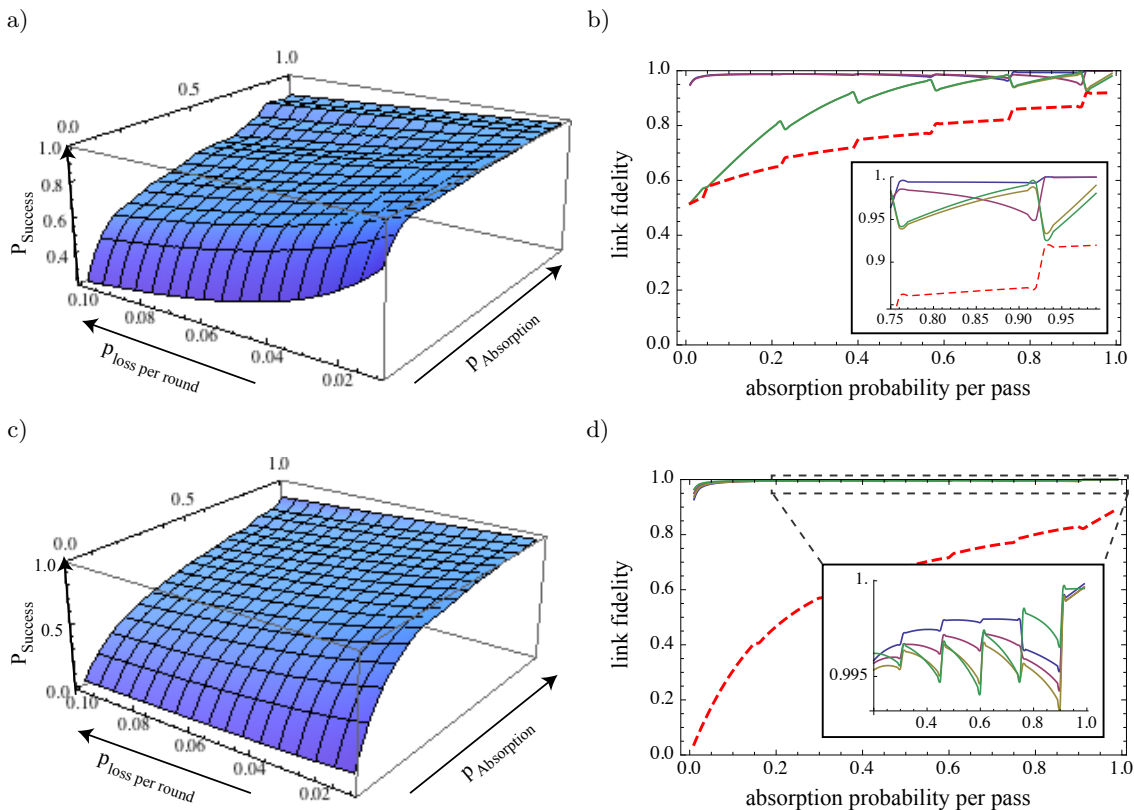


FIG. 4: Success probabilities and fidelities for Approaches A (top) and B (bottom) left: total success probability plotted over probability of absorption and loss per pass. right: Link fidelities for the four possible output Bell states plotted vs. per-pass probability of absorption for a per-pass loss probability of 6.6% (corresponding to 0.3dB). In b and d the insets show a zoom in on the region $p_{\text{abs}} \in [0.75, 1.0]$ (b) and $[0.5, 1.0]$ (d). The meaning of the colours is as in figure 3. The saw-tooth oscillations arise because we can use only discrete (integer) number of rounds with a kink appearing every time we change the number of rounds in our scheme to stay close to the optimum.

V. CONCLUSION

We have presented a proposal for a quantum communications node using only the electronic spin of a nitrogen vacancy center in diamond. It makes use of the Bell-type form of the NV's A_2 state to teleport the link carried by an incoming photon instantly when absorption is heralded by projective QND measurement. The quantum efficiency limit of 25% is overcome by periodically switching the photon's phase and/or polarisation, so that, eventually, all four Bell states are detected. Modelling this scheme as a discrete-time quantum Markov process we were able to obtain a quantitative outline of the expected performance in the presence of some real-world imperfections, foremost among which are photon loss and incomplete absorption per cycle. The results of these simulations suggest, that photon loss per round should be reduced to below 0.5dB while at the same time increasing absorption to 50% per pass or more. If high absorption probabilities can be reached, an approach using a passive phase (polarisation) during each cycle with a final XX (ZZ)-basis measurement would offer the advantage of higher total success probability at comparable

fidelities, provided high-efficiency single photon detectors are available.

VI. ACKNOWLEDGEMENTS

We thank Yuichiro Matsuzaki, Michael Hanks and Remi Blandino for valuable discussions. This research was supported under the Commissioned Research of the National Institute of Information and Communications Technology Quantum Repeater (A & B) project and by a Grant-in-Aid for Scientific Research (A)-JSPS (No. 24244044).

Appendix A: Parameter Estimation Continued

The starting state (2) contains four products of pairwise Bell-states btw. 1 and 3 as well as 2 and p respectively. Only one, $|\psi_{-}\rangle_{2p}$, permits direct transition to $|A_2\rangle$, while the symmetry of the other three matches the other $m_S = \pm 1$ states in the ESM. Since these are split in energy from $|A_2\rangle$ and thus detuned from the

incoming photon, these transitions are suppressed by a Lorentzian factor depending on detuning $\Delta\nu$ and the incoming photon's spectral width $\delta\nu$. The energetically closest state is $|A_1\rangle$ which is split by about 3GHz. Assuming the incoming photon is spontaneously emitted by a remote NV, its lifetime is given by the $|A_2\rangle$ state's lifetime of approximately 10ns. From this the spectral width is $\delta\nu = 1/(10\pi \text{ ns}) \approx 30\text{MHz}$. Thus the transition to the nearest detuned state is already suppressed by a factor $1/(1 + (\Delta\nu/\delta\nu)^2) \approx 10^{-4}$. Transitions to $|E_{1|2}\rangle$ are roughly one order of magnitude smaller still which is why we chose not to include them in our model.

A similar argument can be made to assess the reliability of our QND measurement scheme. Here, there are actually two questions: given the NV center is in A_2 , how certain are we to detect this, and if the system is not in A_2 , but rather still in $m_S = \pm 1$ of the GSM, how likely are we to see a false positive signal? In our model, the former is included in the form of p_{QND} while the latter is part of what we dubbed dark-count probability p_{dark} . As to the first case, the only way not to see a signal is that the system undergoes a transitions to either a dark state or another $m_S = \pm 1$ state. The first cannot occur for a perfect NV center but the possibility grows quadratically with applied strain and electric as well as magnetic fields. All three influences can be reduced to the point where they are negligible: electric fields can be applied to cancel any remaining strain, external magnetic fields can be shielded and flip-flop processes with other spins in the sample, most notably nitrogen P1 centres, are suppressed by the energy splitting in the ESM. Transitions to another state could also be caused the driving field itself, in particular from the starting state in the $m_S = \pm 1$ subspace to $m_S = 0$. However, this can be avoided by choosing the Rabi power such that the Fourier transform of the driving field envelope is zero at this transition frequency (2.88GHz). We therefore choose a conservative $p_{\text{QND}} = 0.99$ and $p_{\text{dark}} = 2 \times 10^{-4}$.

The dephasing times of the NV electronic spin at low temperature have been found to be as long as O(1ms) [] under the right conditions. In our model we assume a commonly seen value of $100\mu\text{s}$ and a total cycle time of $\tau = \tau_{\text{int}} + \tau_{\text{out}} = 200\text{ns}$. The resulting dephasing error per NV involved is therefore $\gamma_2 = 1 - \exp[-(0.005)^2] \approx 4 \times 10^{-6}$. Note that we assume the remote qubits 1 and 3 to be NV centres too, therefore they can be expected to experience the same kind of dephasing. So the worst case dephasing error is then roughly $3\gamma_2$ or 1.2×10^{-5} per cycle.

The absorption probability is the hardest to model since it is very contingent on the sample and technical details of the implementation. Therefore we chose to use it as one of the 'variable' parameters, along with the number of rounds L (both approaches A and B) as well as the phase-and polarisation flip periods l_x and l_z (only approach B).

p_{abs}	$L_{\text{opt.}}$	$P_{\text{false neg.}}^{\text{max}}/q_{\text{QND}}$	$P_{\text{false pos.}}^{\text{max}}/p_{\text{dark}}$
1%	40	0.282	27.5
10%	20	0.836	7.43
25%	20	0.969	2.98
50%	16	0.990	0.999
90%	4	0.9988	0.111

TABLE I: Teleportation scheme errors: the false negative error causes the protocol to discard a teleported link, but even in the interesting regime $p_{\text{abs}} \gtrsim 0.5$ it is never greater than q_{QND}

Appendix B: Teleportation Errors

Here we look at the ways the teleportation scheme can fail within our model and estimate the likelihood for the two types of error: false negatives and false positives.

1. False Negative

In this error scenario we do not see a click heralding teleportation, even though the photon got absorbed (and was subsequently spontaneously re-emitted and then lost) and the entanglement it was carrying was in fact teleported to the remote NV- center 3 (labels as in figure 2). This type of error will cause the whole scheme to fail, since in the absence of a heralding signal node NV2 will demand a new photon to be send from NV1, destroying the entangling link between 1 and 3. Using our discrete model but neglecting (true) dark counts we find an upper bound for the probability of this event

$$\begin{aligned}
 P_{\text{false neg.}}^{\text{max}} &= p_{\text{abs}} q_{\text{QND}} \sum_{l=0}^{L-1} q_{\text{abs}}^l p_{\text{QND}}^l \\
 &= p_{\text{abs}} q_{\text{QND}} \frac{1 - (q_{\text{abs}} p_{\text{QND}})^L}{1 - q_{\text{abs}} p_{\text{QND}}}
 \end{aligned} \tag{B1}$$

with $q_{\text{QND}} \equiv 1 - p_{\text{QND}}$ and $q_{\text{abs}} \equiv 1 - p_{\text{abs}}$. The real value depend on the state ρ_0 but taking this into account can only reduce p_{abs} and thus lead to a lower total error. Using the result from the previous section, App. A, we can set $p_{\text{QND}} \approx 1$ for the range of L that are of interest. Thus (B1) simplifies to $P_{\text{false neg.}}^{\text{max}} \approx q_{\text{QND}}(1 - q_{\text{abs}}^L) \approx q_{\text{QND}}$. The latter approximation holds for the interesting regime $p_{\text{abs}} \gtrsim 0.5$. The results for the exact values of $P_{\text{false neg.}}$ for the different p_{abs} regimes investigated in the main text can be found in third column of table I.

2. False Positive

A false positive error occurs when we see a click that was not actually cause by a correctly detected absorption event but either from a false detection event (proportional to q_{QND} in our model) or a true dark count (p_{Dark}). The latter is a detection event independent of

$p_{\text{absorp.}}$	approach A				approach B							
	L	p_{success}	$F_{\phi_{\pm}}$	$F_{\psi_{\pm}}$	l_z	l_x	L	p_{success}	$F_{\phi_{\pm}}$	$F_{\phi_{-}}$	$F_{\psi_{\pm}}$	$F_{\psi_{-}}$
10%	40	43.3%	0.97	0.89	9	18	36	33.0%	0.993	0.991	0.991	0.990
30%	20	61.6%	0.975	0.97	6	12	24	56.9%	0.995	0.996	0.995	0.996
50%	10	73.8%	0.98	0.97	4	8	16	68.3%	0.996	0.996	0.996	0.997
70%	6	81.7%	0.975	0.97	3	6	12	76.0%	0.996	0.996	0.997	0.998
90%	4	86.9%	0.985	0.99	2	4	8	82.8%	0.997	0.994	0.993	0.995

TABLE II: Single relay performance (success probability and average link fidelities) of the two approaches for different absorption probabilities and choices of total number of rounds L . Photon-loss per cycle was assumed to be .3dB or 6.6%.

anything else. The exact value again depends on the state ρ but we can find an upper bound in a similar manner as for false negatives:

$$\begin{aligned}
P_{\text{false pos.}}^{\text{max}} &= p_{\text{dark}} q_{\text{abs}} \sum_{l=0}^{L-1} q_{\text{abs}}^l q_{\text{dark}}^l \\
&= p_{\text{dark}} q_{\text{abs}} \frac{1 - (q_{\text{abs}} q_{\text{dark}})^L}{1 - q_{\text{abs}} q_{\text{dark}}}
\end{aligned} \tag{B2}$$

Making the approximation $q_{\text{Dark}} \approx 1$ and $q_{\text{abs}}^L \ll 1$, this simplifies to $P_{\text{false neg.}}^{\text{max}} \approx q_{\text{abs}} p_{\text{dark}} / p_{\text{abs}}$. Thus in the in-

teresting absorption regime the overall influence of dark counts is in fact suppressed by the factor $q_{\text{abs}}/p_{\text{abs}} \lesssim 1$. The exact values are given in the fourth column of Table I.

Appendix C: Detailed results

Running simulations varying the number of rounds L and the absorption probability per pas p_{Abs} we found the success probabilities and fidelities given in Table II.

-
- [1] C. H. Bennett and G. Brassard, *Proceedings of IEEE International Conference on Computers, Systems, and Signal Processing*, Bangalore, India, IEEE Press (New York) 175-179 (1984).
 - [2] C.H. Bennett, G. Brassard, S. Popescu, B. Schumacher, J. Smolin and W. K. Wootters, Purification of Noisy Entanglement and Faithful Teleportation via Noisy Channels, *Phys. Rev. Lett.* **76**, 722 - 726 (1996).
 - [3] S. Enk, J.I. Cirac and P. Zoller, Photonic channels for quantum communication, *Science* **279**, 205-208 (1998).
 - [4] N. Gisin, G. Ribordy, W. Tittel and H. Zbinden, Quantum cryptography, *Rev. Mod. Phys.* **74**, 145-195 (2002).
 - [5] N. Gisin and R. Thew, Quantum Communication, *Nature Photon* **1**, 165 - 171 (2007).
 - [6] H. J. Kimble, The quantum internet. *Nature* **453**, 1023-1030 (2008).
 - [7] U. Vazirani and T. Vidick, *Phys. Rev. Lett.* **113**, 140501 (2014).
 - [8] J.I. Cirac, A. Ekert, S. Huelga and C. Macchiavello, Distributed quantum computation over noisy channels. *Phys. Rev. A* **59**, 4249 (1999).
 - [9] R. Van Meter, W. Munro, K. Nemoto and K. Itoh, Arithmetic on a distributed- memory quantum multicomputer, *ACM Journal on Emerging Technologies in Computing Systems* **3**, 2 (2009).
 - [10] V. Giovannetti, S. Lloyd, and L. Maccone, Quantum-Enhanced Measurements: Beating the Standard Quantum Limit, *Science* **306**, 1330 (2004).
 - [11] C.H. Bennett, G. Brassard, C. Crepeau, R. Jozsa, A. Peres, and W.K. Wootters, Teleporting an unknown quantum state via dual classical and Einstein-Podolsky-Rosen channels, *Phys. Rev. Lett.* **70**, 1895 (1993).
 - [12] H.J. Briegel, W. Duř, J.I. Cirac and P. Zoller, Quantum repeaters: The role of imperfect local operations in quantum communication. *Phys. Rev. Lett.* **81**, 5932-5935 (1998).
 - [13] N. Sangouard, C. Simon, N. de Riedmatten and N. Gisin, Quantum repeaters based on atomic ensembles and linear optics, *Rev. Mod. Phys.* **83**, 33-80 (2011).
 - [14] W. Dür, H.-J. Briegel, J. I. Cirac, J. & P. Zoller, Quantum repeaters based on entanglement purification. *Phys. Rev. A* **59**, 169-181 (1999).
 - [15] L. M. Duan, M.D. Lukin, J.I. Cirac, & P. Zoller, Long-distance quantum communication with atomic ensembles and linear optics. *Nature* **414**, 413-418 (2001).
 - [16] P. Van Loock, T. D. Ladd, K. Sanaka, F. Yamaguchi, K. Nemoto, W. J. Munro & Y. Yamamoto, Hybrid quantum repeater using bright coherent light. *Phys. Rev. Lett.* **96**, 240501 (2006).
 - [17] B. Zhao, Z. B. Chen, Y. A. Chen, J. Schmiedmayer & J. W. Pan, Robust creation of entanglement between remote memory qubits. *Phys. Rev. Lett.* **98**, 240502 (2007).
 - [18] Z. Yuan, Y. Chen, B. Zhao, S. Chen, J. Schmiedmayer & J. W. Pan, Experimental demonstration of a BDCZ quantum repeater node. *Nature* **454**, 1098-1101 (2008).
 - [19] A. M. Goebel, G. Wagenknecht, Q. Zhang, Y. Chen, K. Chen, J. Schmiedmayer & J. W. Pan, Multistage Entanglement Swapping. *Phys. Rev. Lett.* **101**, 080403 (2008).

- [20] C. Simon, H. de Riedmatten, M. Afzelius, N. Sangouard, H. Zbinden & N. Gisin, Quantum Repeaters with Photon Pair Sources and Multimode Memories. *Phys. Rev. Lett* **98**, 190503 (2007).
- [21] W. Tittel, M. Afzelius, T. Chanelière, R. L. Cone, S. Kröll, S. A. Moiseev & M. Sellars, Photon-echo quantum memory in solid state systems. *Laser Photon. Rev.* **4**, 244 - 267 (2009).
- [22] N. Sangouard, R. Dubessy & C. Simon, Quantum repeaters based on single trapped ions. *Phys. Rev. A* **79**, 042340 (2009).
- [23] J. W. Pan, S. Simon, C. Brukner & A. Zeilinger, Entanglement purification for quantum communication. *Nature* **410**, 1067-1070 (2001).
- [24] W. Dür & H. J. Briegel, Entanglement purification and quantum error correction. *Rep. Prog. Phys.* **70**, 1381-1424 (2007).
- [25] W. J. Munro, K. A. Harrison, A. M. Stephens, S. J. Devitt & K. Nemoto, From quantum multiplexing to high-performance quantum networking. *Nature Photon.* **4**, 792-796 (2010).
- [26] W. J. Munro, A. M. Stephens, S. J. Devitt, K. A. Harrison and Kae Nemoto, Quantum communication without the necessity of quantum memories, *Nature Photon.* **6** 777 - 781 (2012).
- [27] L. Childress, J. M. Taylor, A. S. Sørensen, and M. D. Lukin. Fault-Tolerant Quantum Communication Based on Solid-State Photon Emitters. *Phys. Rev. Lett.* **96**, 070504 (2006).
- [28] A. M. Stephens, J. Huang, K. Nemoto, and W. J. Munro, *Phys. Rev. A* **87**, 052333 (2013).
- [29] G. Davies and M. F. Hamer. Optical Studies of the 1.945 eV Vibronic Band in Diamond. *Proc. R. Soc. Lond. A* **348**, 285 (1976).
- [30] R. T. Harley, M. J. Henderson, and R. M. Macfarlane. Persistent spectral hole burning of colour centres in diamond. *J. Phys. C* **17**, L233 (1984).
- [31] E. Van Oort, N. B. Manson, and M. Glasbeek. Optically detected spin coherence of the diamond NV centre in its triplet ground state. *J. Phys. C: Sol. Stat. Phys.* **21**, 4385 (1988).
- [32] M. W. Doherty, N. B. Manson, P. Delaney, F. Jelezko, J. Wrachtrup, and L. C. Hollenberg. The nitrogen-vacancy colour centre in diamond. *Physics Reports* **128** (1), 1-45 (2013).
- [33] L. Childress, J. M. Taylor, A. S. Sørensen, and M. D. Lukin, Fault-tolerant quantum repeaters with minimal physical resources and implementations based on single-photon emitters. *Phys. Rev. A* **79**, 052330 (2005).
- [34] M. V. G. Dutt, L. Childress, L. Jiang, E. Togan, J. Maze, F. Jelezko, A. S. Zibrov, P. R. Hemmer, and M. D. Lukin. Quantum Register Based on Individual Electronic and Nuclear Spin Qubits in Diamond. *Science* **316**, 1312-1316 (2007).
- [35] L. Jiang, J. M. Taylor, A. S. Sørensen, and M. D. Lukin. Distributed quantum computation based on small quantum registers. *Phys. Rev. A* **76**, 062323 (2007).
- [36] N. Yao, L. Jiang, A. Gorshkov, P. Maurer, G. Giedke, J. Cirac, and M. Lukin. Scalable Architecture for a Room Temperature Solid-State Quantum Information Processor. *Nature Comm.* **3**, 800 (2012).
- [37] P. C. Maurer, G. Kucsko, C. Latta, L. Jiang, N. Y. Yao, S. D. Bennett, F. Pastawsk, D. Hunger, N. Chisholm, M. Markham, D. J. Twitchen, J. I. Cirac, and M. D. Lukin. Room-Temperature Quantum Bit Memory Exceeding One Second. *Science* **336**, 1283-1286 (2012).
- [38] E. Togan, Y. Chu, A. S. Trifonov, L. Jiang, J. Maze, L. Childress, M. V. G. Dutt, A. S. Sørensen, P. R. Hemmer, A. S. Zibrov, and M. D. Lukin. Quantum entanglement between an optical photon and a solid-state spin qubit. *Nature* **466**, 730-734 (2010).
- [39] F. Jelezko, T. Gaebel, I. Popa, A. Gruber, and J. Wrachtrup. Observation of coherent oscillations in a single electron spin. *Phys. Rev. Lett.* **92**, 076401 (2004).
- [40] T. A. Kennedy, J. S. Colton, J. E. Butler, R. C. Linares, and P. J. Doering, *Apl. Phys. Lett.* **83**, 4190 (2003).
- [41] F. Jelezko, T. Gaebel, M. Domhan, I. Popa, A. Gruber, and J. Wrachtrup, *Phys. Rev. Lett.* **93**, 130501 (2004).
- [42] J. Harrison, M. J. Sellars, and N. B. Manson, *J. Lumin.* **107**, 245 (2004).
- [43] G. Balasubramanian, P. Neumann, D. Twitchen, M. Markham, R. Kolesov, N. Mizuochi, J. Isoya, J. Achard, J. Beck, J. Tissler, et al., *Nature Materials* **8**, 383 (2009).
- [44] G. D. Fuchs, V. V. Dobrovitski, D. M. Toyli, F. J. Heremans, C. D. Weis, T. Schenkel, and A. D. D., *Nature Physics* **6**, 668 (2010).
- [45] Z.-H. Wang, G. de Lange, D. Ristè, R. Hanson, and V. V. Dobrovitski, *Phys. Rev. B* **85**, 155204 (2012).
- [46] P. Neumann, N. Mizuochi, F. Rempp, P. Hemmer, H. Watanabe, S. Yamazaki, V. Jacques, T. Gaebel, F. Jelezko, and J. Wrachtrup, *Science* **320**, 1326 (2008).
- [47] P. Neumann, J. Beck, M. Steine, F. Rempp, H. Fedder, P. Hemmer, J. Wrachtrup, and F. Jelezko, *Science* **329**, 542544 (2010).
- [48] L. Robledo, L. Childress, H. Bernien, B. Hensen, P. F. Alkemade, and R. Hanson, *Nature* **477**, 574 (2011).
- [49] G. Waldherr, Y. Wang, S. Zaiser, M. Jamali, T. Schulte-Herbruggen, H. Abe, T. Oshima, J. Isoya, P. Neumann, and J. Wrachtrup, *Nature* **506**, 204 (2014).
- [50] T. Taminiau, J. Cramer, T. van der Sar, V. Dobrovitski, and R. Hanson, *Nat. Nano.* **9**, 171 (2014).
- [51] E. Togan, Y. Chu, A. S. Trifonov, L. Jiang, J. Maze, L. Childress, M. V. G. Dutt, A. S. Soerensen, P. R. Hemmer, Z. A. S., et al., *Nature* **466**, 730 (2010).
- [52] H. Bernien, B. Hensen, W. Pfaff, G. Koolstra, M. S. Block, L. Robledo, T. H. Taminiau, M. Markham, D. J. Twitchen, L. Childress, et al., *Nature* **497**, 86 (2013).
- [53] H. Kosaka and N. Niikura, *Phys. Rev. Lett.* **114**, 053603 (2015).